AN ANTI-ISLANDING PROTECTION FOR VSM INVERTERS IN DISTRIBUTED GENERATION.

A thesis submitted in partial fulfilment of the requirements for the award of the degree of

B.Tech In

DEPARTMENT OF ELECTRICAL ENGINEERING

By

P.AKSHITHA (B181219)

V.YOGESH (B182448)

G.NEHA (B181137)

K.ANAND KUMAR (B181323)

Under the esteemed Guidance of

Mrs.T.Chaitanya

DEPARTMENT OF ELECTRICAL ENGINEERING

RGUKT, Basar-504107

MAY-2024

BONAFIDE CERTIFICATE

This is to certify that the project titled **AN ANTI-ISLANDING PROTECTION FOR VSM INVERTERS IN DISTRIBUTED GENERATION** is a Bonafide record of the work done by

P.AKSHITHA	**(B181219)**
V.YOGESH	**(B182448)**
G.NEHA	**(B181137)**
K.ANAND KUMAR	**(B181323)**

in partial fulfilment of the requirements for the award of the degree of **Bachelor of Technology** in **ELECTRICAL ENGINEERING** of the **RAJIV GANDHI UNIVERSITY OF KNOWLEDGE TECHNOLOGIES, Basar,** during the year 2023-2024.

Mrs.T.CHAITANYA
Project Guide

Mr.v.VINAY KUMAR
Head of the Department

Project Viva-voce held on 2 -5-2024

Internal Examiner

External Examiner

ABSTRACT

This thesis introduces an innovative anti-islanding protection mechanism tailored for Voltage Source Converter (VSM) inverters within distributed generation systems. The proposed protection system is specifically designed to mitigate the risk of islanding events while ensuring seamless integration and operation of the distributed generation system. The project involves the design, simulation, and experimental validation of anti-islanding algorithms tailored specifically for VSM inverters. Emphasis is placed on real-time detection methods that can swiftly and accurately identify islanding events, triggering the disconnection of the VSM inverter form the grid to ensure gird stability. The proposed anti-islanding protection system is evaluated through simulation studies using advanced modeling techniques to assess its performance under various operating conditions and grid disturbances. The outcomes of this project are expected to contribute to the development of robust anti-islanding protection schemes for VSM inverters, enhancing the safety and reliability of distributed generation systems while facilitating their seamless integration into the existing grid infrastructure.

ACKNOWLEDGEMENT

We thank our project guide Chaitanya madam, for being with us throughout the project and guiding us. We extend our heartfelt gratitude to Our HOD and Faculty for their support. We would also like to thank all our sources, mentioned in the references, and our friends who helped us. This thesis became a reality with the kind support and help of many individuals. I would like to extend my sincere thanks to all of them. I cannot express enough thanks to my committee for their continued support and encouragement .Firstly I would like to express my gratitude to the two main building blocks to the foundation of my project completion namely V.VINAY KUMAR sir (HOD) and T.CHAITANYA madam (Project guide) .I offer my sincere appreciation for the learning opportunities provided by the respected faculties who gave us the possibility to complete this thesis.

The completion of this project could have been accomplished without the support of my team-mates. A special thanks to my teammates who helped me from starting of project to till completion of it. I would also like acknowledge with much appreciation of crucial role of the faculty i,e, our project guide who gave us confidence and encouragement to complete the project and available whenever we struck at our project completion path. Lastly,I would like to appreciate the guidance by the respected faculty and dear friends.With the guidance in our project,we have improved a lot with our presentation skills by the comments and tips given by the respected faculty members.

TABLE OF CONTENTS

LIST OF FIGURES

ABBREVIATIONS

DG - Distributed Generation

VSM- Virtual Synchronous machines

SG- Synchronous generators

AIP- Anti-Islanding protection

PCC- Point of common coupling

PLL- Phase-locked loop

LIST OF TABLES

CHAPTER 1

INTRODUCTION

Over the past decades, renewable energy based distributed generations (DG) are increasing significantly due to the commitment of integration more environment-friendly energy resources. The DGs are connected via power electronics inverters. The virtual synchronous machine (VSM) becomes an attractive solution for controlling these inverters [1]–[4]. The VSM ensures the load sharing naturally in the same way as the conventional synchronous generator (SG) does [5]. Moreover, the VSM control for DG inverters can operate in the grid-connected mode as well as an islanded mode [6]. The operation mode of DG inverters depends upon the state of the main grid. When DG inverters experience an islanding condition (grid absent), they should be disconnected from the rest of the grid in order to avoid personal injury and hazardous operation, and may operate in the islanded mode to supply a local load. The method for detecting and responding to the islanding condition is called anti-islanding protection (AIP) scheme. A proper AIP scheme should be included either in the control of the DG inverters or in the system so that islanding conditions can be detected and the inverters can be disconnected from the rest of the grid in time. It is a desirable feature of the AIP scheme that it should detect the islanding condition accurately and isolate the inverters from the grid as soon as possible when the inverters experience an islanding condition. According to the IEEE Standards 1457, the inverters should be disconnected within 2 s after it experiences an islanding condition [7]. Therefore, embedding an AIP with a high accuracy and less detection time is a requirement for DG inverters. There are many AIP schemes employed in the existing system [8]–[20]. The main challenges in these are the accurate detection of the islanding condition and easy implementation of the AIP scheme. The AIP schemes can be divided into main three categories; communication-based, passive and active AIP schemes. The communication based AIP schemes detect accurately and response quickly in the islanding condition, however, this method suffers from high cost, complicated hardware, and dependence on the communication coverage of their installed location [8], [9]. The passive AIP scheme is mainly realized by employing the over-voltage/under-voltage and overfrequency/ under-frequency. The passive AIP method is simpleand easy to implement, and does not have an impact on the system operation. However, they have a large non-detection zone and suffer from malfunctioning when the local loads are equal to the power supplied by the inverters [10]. In order to overcome these limitations of the passive AIP methods, the fuzzy logic, artificial neural

network, decision trees have been realized. These different techniques give an accurate detection of the islanding condition, however, these schemes become more complicated and difficult in hardware realization [21]. Different active AIP schemes have been proposed in the literature such as correlation-based AIP scheme using current magnitude disturbance [22], harmonic injection method [23], grid impedance estimation method [24]. In these active AIP methods, a small disturbance is injected into the point of common coupling (PCC) to monitor the continuous change in the system parameters. The active AIP methods have a better detection accuracy compared to the passive AIP methods. The main concern of this type of AIP schemes is that these injections may impact the quality of the power supply and introduce the instability problem as well as they require additional devices to inject the disturbance signal [11], [25]. Researches have also been conducted by combining different AIP schemes to achieve a better performance. An AIP scheme based on the combination of a reactive power versus frequency droop and rate of change of frequency is presented in [26]. The scheme is designed so that the reactive power injection is of the minor scale during normal operating conditions. An apparent power-based AIP scheme has been presented in [27] where the detection is based on determining the wavelet packet transform of high-frequency sub-bands present in the d–q-axis components of instantaneous 3-phase apparent powers. This scheme considers an islanding condition if the system creates a non-periodic and non-stationary high frequency component in the apparent power waveform. The active and reactive power variation based AIP scheme is mainly the active method [10], [11], [17], [28]–[30]. In these methods, the active and/or reactive power is injected with a certain frequency into the grid. An example of such an active AIP scheme presented in [28] where the AIP method is based on 40 Hz sinusoidal reactive power injection and used a double- second order generalized integrator topology for computation of harmonic amplitude. The islanding condition is also detected based on the change of the active/reactive power variation in addition to the voltage and/or frequency variation [10], [11]. These methods work well, however, the main concern about these methods is that in an electrical island operation where the voltage and the frequency variation is much higher compared to the grid-connected operation, it causes the inverter to trip. If more inverters are connected in parallel, false trips and stability problems can be experienced. Moreover, the accuracy depends on the selection of the calibration gain Kv and Kf . It is important to execute a correct calibration of Kv to avoid overcurrent. A power line carrier based AIP scheme has been presented in [31]. This AIP scheme mainly relies on transfer trips from upstream substations

through communication media, which are expensive and time-consuming because of the infrastructure. This scheme has been improved by measuring local data only, in which the controller requires a phase-locked loop (PLL) for calculating the firing angle for the thyristor [32]. However, these schemes become more complicated and require additional devices for successful implementation.

The main contribution of this paper is presenting a novel hybrid AIP scheme for the DG inverters. The advantages of this AIP scheme to the existing solutions [8]–[20] are:

Its easy implementation without a need for any additional sensor and power devices in DG inverters;

The AIP scheme is a combination of both active and passive AIP method and does not rely on a communication network;

The complicated disturbance injection method has been avoided, consequently, the risk of triggering instability and power quality issues has been eliminated;

The AIP scheme overcomes the malfunctioning when the local loads are equal to the power supplied by the DG inverter;

The requirements for frequency and phase measurements have been removed.

The AIP scheme detects the islanding condition based on the system parameters such as the active power, the reactive power, and the voltage magnitude mismatches. The AIP scheme detects the islanding condition for all possible operation scenarios and disconnects the inverter from the main grid after it experiences an islanding condition. A detailed operating principle with the analytical modeling of the proposed AIP scheme is presented. Time domain simulations and the experimental results are presented to validate the performance of the proposed AIP scheme for different scenarios such as giving a command signal for changing the reference power of the inverter, initiating an islanding for a case when the local load is equal to the reference power of the inverter, connecting a heavy load, and introducing a grid fault.

In Existing method , Distributed energy resources (DER) such as wind, solar photovoltaic, and energy storage units, are usually connected to the dc micro grid through fast-response power electronic converters. Under the classic control strategy of the interface converters, the kinetic energy stored in the rotor of permanent magnet synchronous generators (PMSG)-based wind turbines and the energy stored in energy storage units cannot be used to slow down the dynamics of dc voltage. In the event of load switching or output fluctuations

of intermittent DERs, dynamic support to the dc voltage can only be provided by dc capacitors As a result, the dc voltage will fluctuate drastically and the stability of the dc micro grid will be reduced. In the proposed system to address the low inertia issue of dc microgrids, several solutions have been proposed. Since the inertia of dc microgrids is mainly provided by dc capacitors, one straightforward way to increase the inertia of dc microgrids is to adopt larger capacitors. In dc microgrids, electrolytic capacitors are usually used as dc capacitors. Due to the disadvantages of electrolytic capacitors, such as bulky volume, low power density and short lifespan, larger dc capacitors are not acceptable for the scale expansion and application of dc microgrids. An approach using D-statcom to improve active and reactive power flow and power oscillation dampings reduced in dc microgrids is presented in this project. Microgrid is a localized grouping of electricity sources and loads that normally operates connected to and synchronous with the traditional centralized electricalgrid (macrogrid), but can disconnect and function autonomously as physical and/or economic conditions dictate. By this way, it paves a way to effectively integrate various sources of distributed generation (DG) especially Renewable Energy Sources (RES). It also provides a good solution for supplying power in case of an emergency by having the ability to change between islanded mode and grid-connected mode. On the other hand, control and protection are big challenges in this type of network configuration, which is generally treated as a hierarchical control.

CHAPTER 2

LITERATURE REVIEW:

In "Equivalence of virtual synchronous machines and frequency-droops for converter-based microgrids,"paper, S. D'Arco and J. A. Suul, explains over the last decade, frequency-droop-based control schemes have become the preferred solution in microgrids dominated by power electronic converters. More recently, the concept of virtual synchronous machines (VSMs) has emerged as an effective method for adding virtual inertia to the power system through the control of power electronic converters. These two approaches have been developed in two separate contexts, but present strong similarities. In fact, they are equivalent under certain conditions, as demonstrated in this letter. Analysis of this equivalence provides additional physics-based insight into the tuning and operation of both types of controllers.

In "Implementation of Hierarchical Control in DC Microgrids,"paper, Y. Hu, R. Zheng, W. Cao, J. Zhang, S. J. Finney, proposed DC microgrids are becoming popular in low-voltage distribution systems due to the better compatibility with photovoltaic panels, electric vehicles, and dc loads. This paper presents a practical dc microgrid developed in the Water and Energy Research Laboratory (WERL) in the Nanyang University of Technology, Singapore. The coordination control among multiple dc sources and energy storages is implemented using a novel hierarchical control technique. The bus voltage essentially acts as an indicator of supply–demand balance. A wireless control is implemented for the reliable operation of the grid. A reasonable compromise between the maximum power harvest and effective battery management is further enhanced using the coordination control based on a central energy management system. The feasibility and effectiveness of the proposed control strategies have been tested by a dc microgrid in WERL.

In "Inertia emulation control strategy for VSC-HVDC transmission systems,"paper "J. Zhu, C. D. Booth, G. P. Adam, A. J. Roscoe, and C. G. Bright," described there is concern that the levels of inertia in power systems may decrease in the future, due to increased levels of energy being provided from renewable sources, which typically have little or no inertia. Voltage source converters (VSC) used in high voltage direct current (HVDC) transmission applications are often deliberately controlled in order to de-couple transients to prevent propagation of instability between interconnected systems. However, this can deny much

needed support during transients that would otherwise be available from system inertia provided by rotating plant.

In “A virtual synchronous machine implementation for distributed control of power converters in smartgrids,”paper “S. D’arco, J. A. Suul, and O. B. Fosso describes the ongoing evolution of the power system towards a “SmartGrid” implies a dominant role of power electronic converters, but poses strict requirements on their control strategies to preserve stability and controllability. In this perspective, the definition of decentralized control schemes for power converters that can provide grid support and allow for seamless transition between grid-connected or islanded operation is critical. Since these features can already be provided by synchronous generators, the concept of Virtual Synchronous Machines (VSMs) can be a suitable approach for controlling power electronics converters. This paper starts with a discussion of the general features offered by the VSM concept in the context of SmartGrids. A specific VSM implementation is then presented in detail together with its mathematical model. The intended emulation of the synchronous machine characteristics is illustrated by numerical simulations. Finally, stability is assessed by analysing the eigenvalues of a small-signal model and their parametric sensitivities.

In “Control of hybrid battery/ultracapacitorenergy storage for stand-alone Photovoltaic system,”paper “X. Liu, P. Wang and P. C. Loh, IEEE, B.P.Baddipadiga,” poposed Battery life is an important criterion in a stand-alone photovoltaic system operation due to intermittent characteristic of solar irradiation and demand. This paper presents a stand-alone photovoltaic system with Ni-MH battery and ultra-capacitor serving as its energy storage elements. A control strategy is proposed in this paper to reduce charging and discharging cycles and avoid deep discharges of battery. The battery converter is controlled in current mode to track a charging/discharging reference current which is given by energy management system, whereas the ultra-capacitor converter is controlled to corporate solar irradiation fluctuations, load spikes and variations to maintain a stable dc-link voltage. Isolated PV system with the proposed control schemes is created using MATLAB SIMULINK. An optimum performance is achieved to serve as both high power and high energy sources due to complementary characteristic of battery and ultra-capacitor.

CHAPTER 3

METHODOLOGY

ENERGY SOURCES

This chapter presents the model, general structure, and control of energy sources considered in the study. This chapter presents an overview of renewable energy sources and their modeling. Each renewable energy source will be developed after validating its design in MATLAB/Simulink.

3.1 SOLAR PHOTOVOLTAIC ENERGY CONVERSION SYSTEM

The photovoltaic effect was experimentally demonstrated first by French physicist Edmond Becquerel. In 1839, at age 19, he built the world's first photovoltaic cell in his father's laboratory. Willoughby Smith first described the "Effect of Light on Selenium during the passage of an Electric Current" in a 20 February 1873 issue of Nature. In 1883 Charles Fritts built the first solid state photovoltaic cell by coating the semiconductor selenium with a thin layer of gold to form the junctions the device was only around 1% efficient. In 1888 Russian physicist Aleksandr Stoletov built the first cell based on the outer photovoltaic effect discovered by Heinrich Hertz in 1887. In 1905 Albert Einstein proposed a new quantum theory of light and explained the photoelectric effect in a landmark paper, for which he received the Nobel Prize in Physics in 1921, Vadim lashkaryov discovered p-n junctions in Cu_2O and silver sulphide protocells in 1941. Russel ohl patented the modern junction semiconductor solar cell in 1946 while working on the series of advances that would lead to the transistor. The first practical photovoltaic cell was publicly demonstrated on 25 April 1954 at Bell Laboratories.

A solar cell, or photovoltaic cell (previously termed "solar battery"[1]), is an electrical device that converts the energy of light directly into electricity by the photovoltaic effect, which is a physical and chemical phenomenon. It is a form of photoelectric cell, defined as a device whose electrical characteristics, such as current, voltage, or resistance, vary when exposed to light. Solar cells are the building blocks of photovoltaic modules, otherwise known as solar panels. Solar cells are described as being photovoltaic, irrespective of whether the source is sunlight or an artificial light. They are used as a photo detector (for example infrared detectors), detecting light or other electromagnetic radiation near the visible range, or measuring light intensity.

3.1.1 OPERATING PRINCIPLE

Solar cells are the basic components of photovoltaic panels. Most are made from silicon even though other materials are also used. Solar cells take advantage of the photoelectric effect: the ability of some semiconductors to convert electromagnetic radiation directly into electrical current. The charged particles generated by the incident radiation are separated conveniently to create an electrical current by an appropriate design of the structure of the solar cell, as will be explained in brief below.

A solar cell is basically a p-n junction which is made from two different layers of silicon doped with a small quantity of impurity atoms: in the case of the n-layer, atoms with one more valence electron, called donors, and in the case of the p-layer, with one less valence electron, known as acceptors. When the two layers are joined together, near the interface the free electrons of the n-layer are diffused in the p-side, leaving behind an area positively charged by the donors. Similarly, the free holes in the p-layer are diffused in the n-side, leaving behind a region negatively charged by the acceptors.

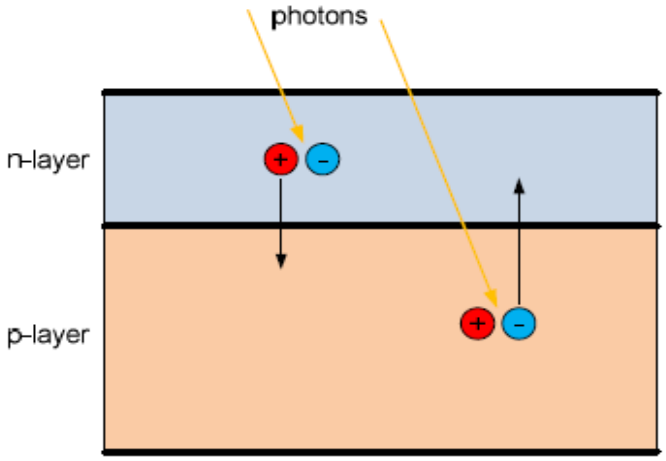

Fig.1 Solar cell.

This creates an electrical field between the two sides that is a potential barrier to further flow. The equilibrium is reached in the junction when the electrons and holes cannot surpass that potential barrier and consequently they cannot move. This electric field pulls the electrons and holes in opposite directions so the current can flow in one way only: electrons can move from the p-side to the n-side and the holes in the opposite direction. A diagram of the p-n junction showing the effect of the mentioned electric field is illustrated in Fig.2.1. Metallic contacts are added at both sides to collect the electrons and holes so the current can flow. In the case of the n-layer,

which is facing the solar irradiance, the contacts are several metallic strips, as they must allow the light to pass to the solar cell, called fingers. The structure of the solar cell has been described so far and the operating principle is next. The photons of the solar radiation shine on the cell. Three different cases can happen: some of the photons are reflected from the top surface of the cell and metal fingers. Those that are not reflected penetrate in the substrate. Some of them, usually the ones with less energy, pass through the cell without causing any effect. Only those with energy level above the band gap of the silicon can create an electron-hole pair. These pairs are generated at both sides of the p-n junction. The minority charges (electrons in the p-side, holes in the n-side) are diffused to the junction and swept away in opposite directions (electrons towards the n-side, holes towards the p-side) by the electric field, generating a current in the cell, which is collected by the metal contacts at both sides. This can be seen in the Fig.2.1. This is the light-generated current which depends directly on the irradiation: if it is higher, then it contains more photons with enough energy to create more electron-hole pairs and consequently more current is generated by the solar cell.

3.1.2 EQUIVALENT CIRCUIT OF A SOLAR CELL

The solar cell can be represented by the electrical model shown in Fig.2.2. Its current voltage characteristic is expressed by the following Eqn.(2.1).

$$I = I_L - I_O\left(e^{\frac{q(v-IR_S)}{AKT}} - 1\right) - \frac{V - IR_S}{R_{SH}} \dots (2.1)$$

Where I and V are the solar cell output current and voltage respectively, I0 is the dark saturation current, q is the charge of an electron, A is the diode quality (ideality) factor, k is the Boltzmann constant, T is the absolute temperature and R_S and R_{SH} are the series and shunt resistances of the solar cell. R_S is the resistance offered by the contacts and the bulk semiconductor material of the solar cell. The origin of the shunt resistance R_{SH} is more difficult to explain. It is related to the non ideal nature of the p–n junction and the presence of impurities near the edges of the cell that provide a short-circuit path around the junction. In an ideal case R_S would be zero and R_{SH} infinite. However, this ideal scenario is not possible and manufacturers try to minimize the effect of both resistances to improve their products.

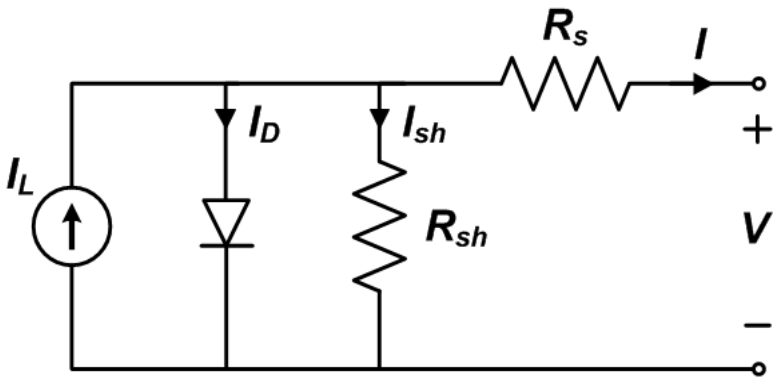

Fig.2 Equivalent circuit of a solar cell.

Sometimes, to simplify the model, as in the effect of the shunt resistance is not considered, i.e. R_{SH} is infinite, so the last term in Eqn.(2.1) is neglected. A PV panel is composed of many solar cells, which are connected in series and parallel so the output current and voltage of the PV panel are high enough to the requirements of the grid or equipment. Taking into account the simplification mentioned above, the output current-voltage characteristic of a PV panel is expressed by Eqn.(2.2), where n_p and ns are the number of solar cells in parallel and series respectively.

$$I = n_p I_L - n_p I_O \left(e^{\frac{q(v - IR_S)}{AKTn_s}} - 1 \right) \ldots (2.2)$$

3.1.3 OPEN CIRCUIT, SHORT CIRCUIT CURRENT AND MAXIMUM POWER POINT

Two important points of the current-voltage characteristic must be pointed out: the open circuit voltage V_{OC} and the short circuit current I_{SC}. At both points the power generated is zero. V_{OC} can be approximated from Eqn.(2.1) when the output current of the cell is zero, i.e. I=0 and the shunt resistance R_{SH} is neglected. It is represented by Eqn.(2.3). The short circuit current I_{SC} is the current at V = 0 and is approximately equal to the light generated current I_L as shown in Eqn.(2.4).

$$V_{OC} = \frac{AKT}{q} ln \left(\frac{I_L}{I_O} + 1 \right) \ldots (2.3)$$

$$I_{SC} = I_L \ldots (2.4)$$

The maximum power is generated by the solar cell at a point of the current-voltage characteristic where the product VI is maximum. This point is known as the MPP and is unique, as can be seen in Fig.2.3, where the previous points are represented.

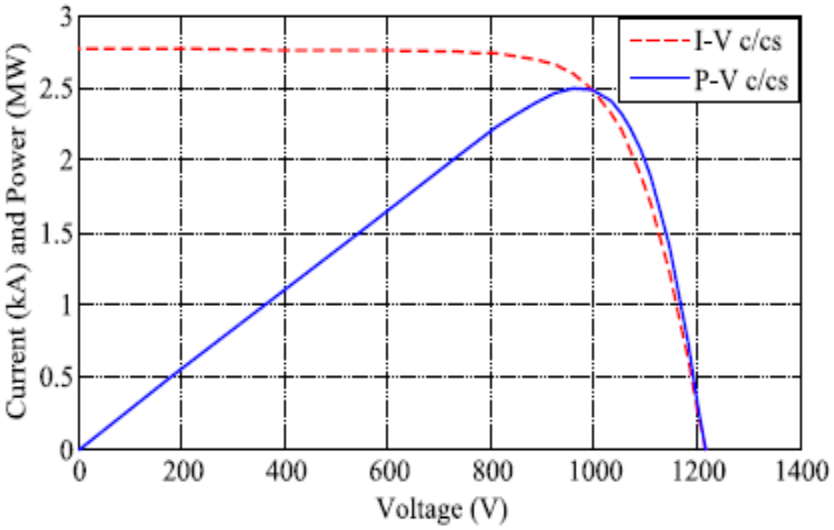

Fig.3 Important points in the characteristic curves of a solar panel.

3.1.4 FILL FACTOR

Using the MPP current and voltage, I_{MPP} and V_{MPP}, the open circuit voltage (V_{OC}) and the short circuit current (I_{SC}), the fill factor (FF) can be defined as:

$$FF = \frac{I_{MPP}V_{MPP}}{I_{SC}V_{OC}} \ldots (2.5)$$

It is a widely used measure of the solar cell overall quality. It is the ratio of the actual maximum power ($I_{MPP}V_{MPP}$) to the theoretical one ($I_{SC}V_{OC}$), which is actually not obtainable. The reason for that is that the MPP voltage and current are always below the open circuit voltage and the short circuit current respectively, because of the series and shunt resistances and the diode depicted in Fig.2.2, The typical fill factor for commercial solar cells is usually over 0.70.

As was mentioned before, the temperature and the irradiation depend on the atmospheric conditions, which are not constant during the year and not even during a single day; they can vary rapidly due to fast changing conditions such as clouds. This causes the MPP to move constantly, depending on the irradiation and temperature conditions. If the operating point is not close to the MPP, great power losses occur. Hence it is essential to track the MPP in any conditions to assure that the maximum available power is obtained from the PV panel. In a modern solar power converter, this task is entrusted to the MPPT algorithms.

3.2 POWER MANAGEMENT STRATEGIES

Since the study includes the operation of energy system consisting solar energy systems, following topics are considered in developing the simulation model:

i. Feasibility studies

ii. Solar photovoltaic energy conversion systems

iii. Maximum power point tracking systems and PI controller

3.2.1 Feasibility Study

One of the recent studies on the feasibility of a standalone solar-wind hybrid energy system for application in the region of Ethiopia shows a potential of such systems. According to the reference, the annual average irradiation in Europe is about 1000 kWh/m2, in middle-east it's approximately around 1800 kWh/m2. In the tropical zone the average is estimated to be around 2000 kWh/m2. Based on a variety of design parameters; such as PV size, wind turbine rotor swept area, battery capacity, PV module slope angle, and wind turbine installation height leveled cost of energy ($/kW h) ranging in between $1 and $4 have been estimated.

The installation of solar energy system in remote areas is one of the promising applications of renewable energy technology. Recent research and development of have shown excellent potential, as a form of supplementary contribution to conventional power generation system. PV energy system reduces the requirement of a battery bank and a diesel engine. Feasibility of PV energy system strongly depends on solar radiation and wind energy potential available at the site. Optimum size of PV energy system can be calculated on an hourly basis or on the basis of daily average power per month, the day of minimum PV power per month, and the day of minimum wind power per month. In the conventional approach power electronics based DC–DC converter are used for maximum energy extract from solar energy sources and control the complete hybrid system. Some researchers in have used different controlling technique for different combination of energy systems.

The study in proposed an advanced control technique to manage the flow of energy efficiently with good power quality. The system voltage variation, the frequency, waveform and power factor at the time of grid connection, must be maintained within the limits. Hybrid energy flow can also be controlled by applying advance control techniques on power electronic

converters. Another study in focuses on the application status and outlook of wind–solar hybrid energy system in China. The density of potential wind energy is more than 50 W/m2. Wind–solar hybrid energy system is more and more considered in China as a renewable energy resource compared to conventional stand-alone wind energy system and solar energy system. The circuit topology must be regarded to acquire the maximum power point (MPP). The conventional buck, boost and buck-boost circuit are used in the hybrid system, but the efficiency is low during the acquire MPP course.

It says that some intelligent control method must be used to improve the conventional proportional-integral-derivative (PID) controller to develop an advance MPPT algorithm. The efficient MPPT algorithm must be considered to increase the output efficiency of generate system. The study in states that the climatic conditions determine the availability and magnitude of solar and wind energy at particular site. The long term performance is one of the most important design criteria for stand-alone hybrid energy systems. So, weather data containing hourly solar irradiation, and ambient temperature are required for feasibility study and design of RES systems.

3.2.2 Solar Photovoltaic Energy Conversion Systems

For the generation of electricity in remote area at reasonable price, sizing of the power supply system plays an important role. Since the scaling of input power source is easy, solar PV systems are an excellent choice in remote areas for low and medium level power generation. According to a provisional design specification of TechnoCentre Éolien, a 5kW solar PV system was proposed and was integrated in hybrid energy system configuration. The given structure is this study was a standard configuration used for conventional solar PVECS. That includes a solar PV array, DC-DC buck converter, MPPT controller and loads connected through a controlled DC-AC three phase inverter. The generation side DC-DC converter is controlled with signals from maximum power point tracking (MPPT) system and the grid or load side converter is controlled with a two-level VSC.

There are two major families of PV generation system as described:

i. Grid-connected system

ii. Stand-alone system

In this research, a simulation model of stand-alone microgrid is developed based on the infrastructure in TechnoCentre Éolien. Most usual configuration of stand-alone PV system comes with an energy storage system. The building block of PV array is solar cell, which is basically a p-n semiconductor junction that directly converts solar irradiation into DC current using the photovoltaic effect. A mathematical model of solar PV cell can be obtained from the equivalent circuit. The PV module was constructed with a number of solar cells in series-parallel connection and a number of PV modules are required to make an array.

3.2.3 Maximum Power Point Tracking Algorithm

Maximum power point tracking is a technique that ensures the maximum power extraction from non-linear energy resources like solar photovoltaic, wind energy systems and tidal energies. For solar PV systems, MPPT algorithm allows the controller to follow the optimum voltage and current from a photovoltaic module. Most widely used MPPT algorithms are:

a. Constant voltage method

b. Perturb & Observe (P&O) method

c. Incremental conductance method

a. Constant Voltage Method

Although this method is very simple, it is always difficult to select the optimal value of constant *K*, which reduces the efficiency of power generation. The basis of the constant voltage algorithm is an observation from current-voltage (I-V) characteristic curve, the ratio of the PV array's maximum power voltage, VMPP to its open-circuit voltage, VOC that is approximately constant. In other words: $(VMPP / VOC) \approx K < 1$. The MPPT calculates the correct operating point using this relationship between VMPP & VOC and adjusts the array voltage until it reaches the MPP with a pre-set value of *K*. The operation is repeated periodically to track the MPP position.

b. Perturb & Observe (P&O) Method

This method is also known as Hill Climbing (HC) method. Its working principle is making a small active voltage perturbation in a certain working voltage of photovoltaic cells and observing the change direction of output power. Disturbance observation has been widely used in photovoltaic maximum power point tracking because of its simple control structure. However, due

to its fixed step, the oscillation phenomenon occurs near the maximum power point, which reduces the efficiency of power generation. In the P&O algorithm, the operating voltage of the PV array is perturbed by a small increment, and the resulting power change (ΔP) is measured. If ΔP is positive, then the perturbation of the operating voltage moved the PV array's operating point closer to the MPP. The advantage of this method is its simplicity and that is easy to implement. The P&O method has a limitation to track the MPP when the sunlight decreases, because the power-voltage (P-V) characteristic curve flattens out. Another fundamental drawback of P&O method is that it cannot determine when it has actually reached the MPP.

c. Incremental Conductance Method

This method estimates the relation between the operating point voltage, *U* and the maximum power point voltage, *Umax*. The method of increasing conductivity follows three conditions: $U < Umax$, $U > Umax$ *and* $U = Umax$. To realize the position of maximum power point a reference voltage *Uref* is applied. For a light intensity and outside temperature variation, the incremental conductance method could control the output voltage to track the maximum power point voltage smoothly and could also reduce oscillation phenomena near the maximum power point. However, this control algorithm is very complex, and the setting of adjusting voltage ΔU influences the maximum power point tracking accuracy greatly. In another study a terminal sliding mode control (TSMC) algorithm has been applied to achieve the MPP under the changing atmosphere. Here, a module current *(ipv*) and a voltage (*Vpv)* are measured from PV array and sent to the MPP searching algorithm that generates the reference maximum power voltage, *Vpvd*. Then, the reference voltage, *Vpvd*, is given to the MPV-based TSMC algorithm for the maximum power tracking.

	Constant Voltage (CV)	*Perturb & Observe (P&O)*	*Incremental Conductance*
Method	Open Circuit Voltage	Hill Climbing	Hill Climbing
Response Time	Fast	Faster	Slow
Efficiency (approx.)	73-85%	81.5-85%	88-89.9%
Accuracy	Low	High	Higher

Table 1 Comparison between the types of MPPT algorithms

To achieve the maximum power tracking, the terminal sliding mode controller is proposed to let PV voltage *Vpv* track the reference MPV *Vpvd*. The incremental conductance algorithm starts with measuring the present values of PV module voltage, *V*, and current, *I*. Then, it calculates the incremental changes in current *(dI)* and voltage *(dV)* using the present values of current and voltage respectively. The incremental conductance algorithm is derived by differentiating the PV array power with respect to voltage and setting the result equal to zero. A primary advantage of the incremental conductance over the perturb-and-observe algorithm is that the incremental conductance can actually calculate the direction in which to perturb the array's operating point to reach the MPP. It can determine when it has actually reached the MPP. Thus, under rapidly changing conditions, it should not track in the wrong direction, as P&O can, and it should not oscillate about the MPP once it reaches it. Based on the above literature review on MPPT algorithms for solar PV systems, a comparative analysis between the methods is summarized below.

3.3 MICROGRID

Low and medium DG network is in quick improvement around the world. They are controlled by sustainable, non-regular generators which incorporate; power modules, wind turbines, and photovoltaic network (Li et al., 2004; Chowdhury et al., 2009). Regularly, they are utilized to increase the utility network amid pinnacle hour stack, where that time compares to a deficiency of energy. They can likewise offer help to control in cases the fundamental network lattice falls flat. As of late, the idea has become all the more intriguing where the gathering of a course of action

of burdens framing a bunch, together with parallel DG units, constitutes what is known as a Microgrid. Little generators can be joined into the power network, as in the conventional technique where a little generator unit was meant to decrease the effect of network operation in each interconnected microsource. For a blackout in the grid organize because of a mistake identified in the utility lattice, it will efficiently influence and close down the generator units, contrasted with a Microgrid when the network system is off, the power close down, the Microgrid will methodicallly disengage from the lattice arrange and works autonomously in giving energy to its neighborhood stack when the utility has returned to typical.

3.3.1 MICROGRID BENEFITS

The advancement of Microgrid fills in as a method for picking up favorable position contrasted with different networks, this is explained below (Chowdhury et al., 2009):

- As of natural concerns, a Microgrid chops down contamination since it utilizes microsource that deliver low or zero discharges.
- Microgrids work in parallel to the utility Grid; by dealing with specific burdens they bolster the utility network. The additional limit given by Microgrids can help avoiding over-burden circumstances and power outages of the national grid.
- Economically, there is diminishment in long transmission line establishment and the comparing transmission. The minimal effort establishment of the Microgrid networks locally impressively spares foundation expenses and transmission misfortunes. Microgrids additionally help in decreasing the utilization of fossil energy.
- By working in both grid associated and islanded mode, it guarantees uninterruptable burdens. This makes it more solid and conveys superb energy to the basic loads.
- The Microgrid exploits heat energy sparing when utilizing combined heat and power. This is a simple procedure to accomplish with the micro source in a Microgrid. The microsource can be sent nearer to heat and electrical loads for amplifying energy proficiency.
- The Microgrid exploits heat energy sparing when utilizing combined heat and power. This is a simple procedure to accomplish with the microsource of a Microgrid. For boosting energy effectiveness, the microsource can be conveyed nearer to the heat and electrical loads.

3.4 TECHNICAL IMPACTS OF MICROGRIDS ON THE DISTRIBUTION SYSTEM

Network voltage changes and system regulation

Each conveyance utility has a commitment to supply its clients power at a voltage inside a predetermined breaking point. This prerequisite frequently decides the plan and cost of the dissemination circuit so that throughout the years procedures have been created to make the greatest utilization of appropriation circuits to supply clients inside the required voltage. Some circulation utilities utilize more advanced control of the on load tap changers of the dissemination transformer by controllers on the feeder and including the utilization of the present flag intensified with the voltage estimation at the exchanged capacitor on feeders.

Increase of network fault levels

The majority of the Microgrid plants utilize turning machines and these will add to the system blame levels. Both enlistment and synchronous generators will expand the blame level of the dispersion network despite the fact that their conduct under supported blame conditions contrasts. The blame level commitment can be diminished by presenting impedance between the generator and the system by a transformer or reactor however to the detriment of expanded misfortunes and more extensive voltage varieties at the generator. In urban regions where the current blame level methodologies the rating of the switchgear, the expansion in blame level can be a genuine obstacle to the advancement of Distributed Generation.

Power quality

Two parts of energy quality are generally thought to be essential: (i) transient voltage varieties and (ii) consonant twisting of the system voltage. The Microgrid can bring about transient voltage minor departure from the system if generally vast current changes amid association and disengagement of the generator are permitted. In this manner, it is important to utmost voltage varieties to limit the light variety. Large stack vacillation can bring about voltage variety and additionally source change. Microgrid units can possibly bring about undesirable transient voltage varieties at the neighborhood control network.

Step changes in the yields of the Microgrid units with regular vacillations and the communication between the Microgrid and voltage controlling gadgets in the feeder can bring about noteworthy voltage varieties. The independent operation of Microgrid units gives more

potential for voltage varieties because of load unsettling influences, which make sudden current changes the DG inverter. In the event that the yield impedance of the inverter is sufficiently high, the adjustments in the present will bring about noteworthy changes in the voltage drop, and therefore, the AC yield voltage will vacillate. On the other hand, frail ties in the network mix mode give a possibility for transient voltage varieties to happen yet bring down degrees than in the independent mode.

Protection

Various diverse parts of Microgrid assurance can be recognized:

- Protection of the era gear from interior flaws.
- Protections of the blamed dissemination organize from blame streams provided by the Microgrids.
- Anti-islanding or loss-of-mains insurance.
- Impact of Microgrids on existing dispersion network insurance.

Stability

For Distributed Generators conspires, the target of which is to produce control from new sustainable power sources, contemplations of generator transient solidness tend not to be of awesome essentialness. In the event that blame happens some place in the appropriation system to discourage the system voltage and the Distributed Generator trips, then all that is lost is a brief time of era. The Microgrids will keep an eye on over speed and stumble on their interior security. The controls conspire in the Microgrids will then sit tight for the system condition to be reestablished and restart consequently. Interestingly, if a DG is seen as offering help for the power network, then its transient dependability is the fate of extensive significance. Both voltage and potentially point solidness might be noteworthy relying upon the conditions.

3.5 TYPES OF MICROGRIDS

1) Campus Environment/Institutional Microgrids

The concentration of grounds Microgrids totally existing in nearby era with different burdens that is situated in tight geology in which proprietor effortlessly oversee them.

2) Remote "Off-Grid" Microgrids

These Microgrids never interface with the Macrogrid and rather work in an island mode at all circumstances in light of temperate issue or topography position. Commonly, an "off-Grid" Microgrid is inherent zones that are far removed from any transmission and conveyance foundation and in this manner have no association with the utility network.

3) Military Base Microgrids

These Microgrids are as a rule effectively sent with concentrate on both physical and digital security for military offices keeping in mind the end goal to guarantee dependable power without depending on the Microgrid.

4) Commercial and Industrial (C&I) Microgrids

These sorts of Microgrids are developing rapidly in North America and Asia Pacific; be that as it may, the absence of well –known models for these sorts of Microgrids cutoff points them universally. Primary purposes behind the establishment of a modern Microgrid are power supply security and its unwavering quality. There are many assembling forms in which an interference of the power supply may bring about high income misfortunes and long start-up time.

3.4.1 BASIC COMPONENTS IN MICROGRIDS

Local generation

It presents different sorts of era source that encourage power to client. These sources are partitioned into two noteworthy gatherings – ordinary vitality sources (ex. Diesel generators) and inexhaustible era sources (e.g. wind turbines, sunlight based).

Consumption

It essentially alludes to components that devour power which extend from single gadgets to lighting, warming arrangement of structures, business focuses, and so on. On account of controllable burdens, the power utilization can be adjusted popular of the system.

Energy Storage

In Microgrid, vitality stockpiling can play out numerous capacities, for example, guaranteeing power quality, including recurrence and voltage control, smoothening the yield of sustainable power sources, giving reinforcement energy to the network and assuming critical part

in cost enhancement. It incorporates all of electrical, weight, gravitational, flywheel, and warmth stockpiling innovations.

Point of basic coupling (PCC)

It is the point in the electric circuit where a Microgrid is associated with a fundamental grid. Microgrids that don't have a PCC are called confined Microgrids which are typically exhibited on account of remote locales (e.g., remote groups or remote mechanical destinations) where an interconnection with the primary network is not doable because of either specialized as well as financial imperatives.

3.6 ANALYTICAL MODELING AND OPERATION PRINCIPLE OF THE PROPOSED AIP SCHEME

The proposed hybrid AIP method is based on the detection of active power, reactive power and voltage mismatch, which is shown to be an alternative to the impedance variation measurement technique. The analytical modeling and its implementation presented in the following section.

A. ANALYTICAL MODELING OF THE AIP IMPLEMENTATION

Fig. 1 shows a DG inverter and its VSM controller in a general form. The inverter sends the active power, P and the reactive power, Q to the grid according to its set power Pset and Qset . It is important to note that in this work, the inverter currentis used to calculate the active and reactive power as shown in Fig. 1. The power of the inverter can be given by

$$P = P_{set} = \frac{V_o^2}{R_T} \qquad (1)$$

$$Q = Q_{set} = V_o^2 \left(\frac{1}{2\pi f_1 L_T} - 2\pi f_1 C_T \right) \qquad (2)$$

where Vo is the capacitor voltage magnitude, f1 is the fundamental frequency, RT , LT andCT are the equivalent resistance, inductance and capacitance respectively. If there are multiple DG sources connected to the PCC, (1) and (2) are still valid since each of DG source has its own equivalent RT , LT and CT .

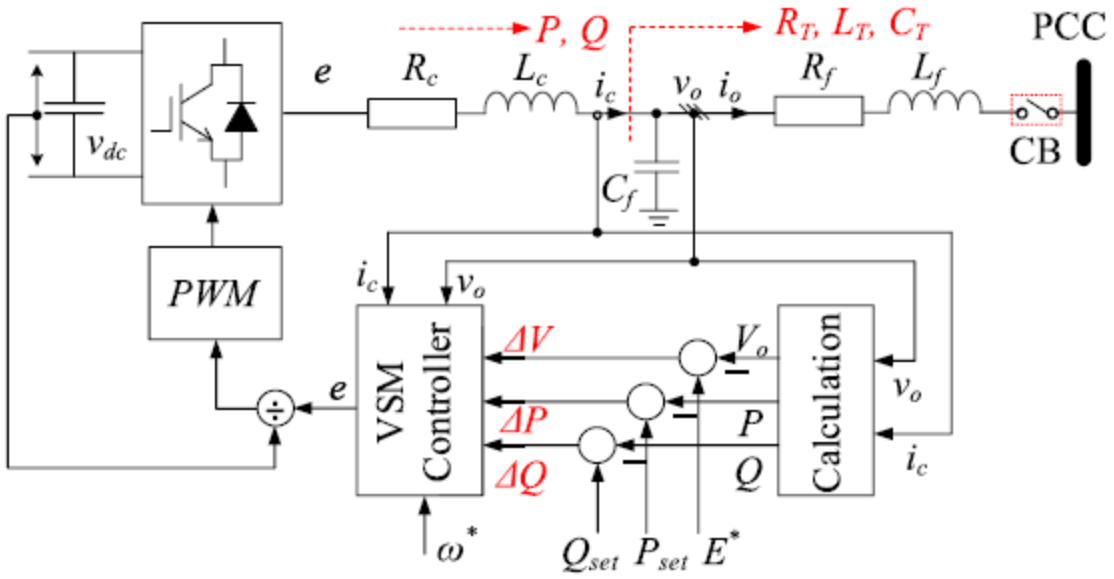

FIGURE 4. A general form of a VSM-based DG inverter and it's controller.

In the grid-connected mode, the grid mainly regulates the voltage and frequency, and the DG inverters transfer power to the grid based on its reference power, Pset and Qset . However, in the islanded mode, the DG inverters take part in the voltage and frequency regulation and send power P and Q based on the connected local load, i.e., equivalent RT , LT andCT . Since the inverters do not send the power according to its Pset and Qset in the islanding condition, there is a power mismatch between the set power and actual power. This power mismatch can be given by

$$\Delta P = P_{set} - P \qquad (3)$$

$$\Delta Q = Q_{set} - Q. \qquad (4)$$

Eqns. (1) and (2) indicate that the power mismatch from the grid-connected mode to an islanding condition results from a change ofVo, f , and connected load, i.e., RT , LT andCT . From (1) and (2), the power mismatch can be given by

$$\Delta P = \frac{2V_o}{R_T}\Delta V_o - \frac{V_o^2}{R_T^2}\Delta R_T. \quad (5)$$

$$\Delta Q = 2V_o\left(\frac{1}{2\pi f_1 L_T} - 2\pi f_1 C_T\right)\Delta V_o - \frac{V_o^2}{2\pi f_1 L_T^2}\Delta L_T - 2\pi f_1 V_o^2 \Delta C_T - V_o^2\left(\frac{1}{2\pi f_1^2 L_T} + 2\pi C_T\right)\Delta f. \quad (6)$$

The Delta symbol Δ is used to represent a variation of the parameters from the grid-connected operation to an islanding condition, for example, the equivalent resistance is RT in the grid-connected operation when in an islanding condition, it is RT +ΔRT . Both the grid-connected mode and the islanded mode, the voltage and frequency are regulated by controlling the generation of the active and reactive power, therefore, ΔVo and Δf can be disregarded in (5) and (6). Thus, the power mismatches can be expressed as

$$\Delta P = -\frac{V_o^2}{R_T^2}\Delta R_T \quad (7)$$

$$\Delta Q = -\frac{V_o^2}{2\pi f_1 L_T^2}\Delta L_T - 2\pi f_1 V_o^2 \Delta C_T. \quad (8)$$

Detection of an islanding condition by monitoring the grid impedance variation is a very effective active AIP technique [19], [24]. The impedance variation is obtained by a perturbation method where a harmonic current (ih,i) or voltage (vh,i) signal is injected at the PCC, and the impedance is obtained from responses of the corresponding harmonic voltage (vh,r) or current (ih,r) with respect to injected signal as

$$Z_h = v_{h,r}/i_{h,i} = v_{h,i}/i_{h,r}. \quad (9)$$

The main concern is this method requires additional devices to inject the perturbation signal and more computational effort is needed in real-time impedance calculation. Eqns. (7) and (8) indicate that the power mismatch is proportional to the grid impedance variation. As shown in Fig. 1, ΔP

and ΔQ, which is equivalent to the impedance variation, can be obtained directly from the controller without injection of a disturbance signal. If the inverter is connected to the grid, P and Q follow Pset and Qset . Hence, the power mismatch in (7) and (8) is zero, which meaning ΔRT = ΔLT = ΔCT = 0 in (7) and (8). However, during the change of operation condition from grid-connected mode to an islanding condition, ΔRT , ΔLT and ΔCT will not be zero [24], resulting in a mismatch in the active power and reactive power. The inverter usually operates under close to the unity power factor and the reactive power Qset is usually set to zero when the inverter is connected to the grid. However, in an islanding condition, the inverter supplies or absorbs the reactive power depending on the connected LT and CT . For example, an unloaded transmission line connected to the inverter in the islanding condition generates the reactive power while an unloaded transformer absorbs the reactive power. The inverter maintains the voltage and frequency at the reference set point by absorbing or generating the reactive power and the active power. Therefore, there must be a mismatch between the set reactive power Qset and the supplied reactive power Q from the inverter in an islanding condition. The reactive power mismatch is considered to be the first criterion for detecting an islanding condition. In the islanding condition, the reactive power mismatch ΔQ exceeds a threshold limit, QL with a typical value of 0.1 pu, i.e., (10) is satisfied.

$$| \Delta Q | \geq Q_L \qquad (10)$$

The second condition is about the mismatch of the active power. If the active power mismatch ΔP exceeds a threshold limit, PL with a typical value of 0.1 pu, i.e., (11) is satisfied in the islanding condition.

$$| \Delta P | \geq P_L \qquad (11)$$

The DG inverter supplies or absorbs the power to regulate the voltage and frequency in an island operation. If the inverter output current reaches its limit, it can no longer increase its power to maintain the voltage as a result, the voltage magnitude will tend to exceed from its operating range 0.95-1.05 pu. The voltage mismatch defined by

$$\Delta V = E^* - V_o \qquad (12)$$

where E∗ is the rated voltage, may exceed from the standard operating range. In severe cases, a voltage instability/collapse may occur. Hence, in addition to the power mismatch, the voltage mismatch has been considered as another condition for the AIP scheme if ΔV exceeds the threshold limit VL, i.e., (13) is satisfied.

$$| \Delta V | \geq V_L, \qquad (13)$$

The logic in the AIP scheme is set in such a way that if the condition in (10) is satisfied and together with at least one of the conditions from (11) and (13), the AIP scheme assumes the situation as an islanding condition.

B. CRITICAL CASE SCENARIO

The critical case is defined for the case when the inverter power becomes equal to the local load power in an islanding condition. Based on the discussion in the previous subsection, the AIP scheme proposed is based on the monitoring of the system parameters mismatch, therefore, it is a passive AIP scheme. Though the passive method is easy implementation, the challenge is: it cannot detect an islanding condition when the local load power, Pload is equal to Pset , i.e., Pset = P = Pload . Under this condition, the second criterion in (11) will not be fulfilled in an islanding condition since

$$| \Delta P | = | P_{set} - P_{load} | \approx 0 \leq P_L. \qquad (14)$$

The inverter regulates the voltage in an islanding condition, therefore, the voltage stays within the limit, thus, (13) will not be satisfied as well. Since in addition to (10) at least one of the conditions from (11) and (13) need to be satisfied in the proposed AIP scheme, this method may fail to detect an islanding condition when Pset = Pload . In order to avoid this failure, the AIP scheme is altered to an active AIP scheme when only (10) is satisfied. An active power injection is applied in order to avoid a potential instability problem. The AIP scheme sends a command signal to the inverter for changing the active power set point. A step reduction of reference power, ΔPset is applied, for which new power set point becomes (Pset − ΔPset). Hence, the new power mismatch can be given by

$$\Delta P = (P_{set} - \Delta P_{set}) - P_{load} = -\Delta P_{set}. \qquad (15)$$

Pset should be higher than threshold limit. The active power mismatch in (11) is forced to exceed the threshold limit by giving the command for changing the active power reference of the inverter. If the inverter operates in the grid-connected mode, changing the active power reference will not lead to the threshold surpass since P will follow the power reference. Under an islanding condition, the inverter will supply the power equal to the local load power, and the inverter will not follow the command of the power reference change, ΔP_{set} . The command signal for changing the power reference from Pset to $P_{set} - \Delta P_{set}$ will force to have an active power mismatch equivalent $|\Delta P| = |\Delta P_{set}|$ and exceed the threshold limit. Hence, in addition to the reactive power mismatch condition of (10), the active power mismatch in (11) will be satisfied. It can also be likely to happen in an islanding condition that the set reactive power is equal to the total connected reactive power load, i.e., $Q_{set} = Q = Q_{load}$. Under such critical case scenarios, to avoid the undetected condition, a step reduction of reference reactive power, ΔQ_{set} is applied, for which new reactive power set point becomes $(Q_{set} - \Delta Q_{set})$. Hence, the new reactive power mismatch can be given by $\Delta Q = (Q_{set} - \Delta Q_{set}) - Q_{load} = -\Delta Q_{set}$. ΔQ_{set} should be higher than threshold limit. The reactive power is forced to exceed the threshold limit by giving the command for changing the reactive power reference of the inverter. Hence, in addition to the active power mismatch condition in (11), the reactive power mismatch in (11) will be satisfied. Thus, the AIP scheme will detect an islanding condition.

C. AVOIDING A FAULT TRIGGERING

Many other cases such as a grid fault, voltage drop, frequency drop, different transient phenomena could cause a power and voltage mismatch for a short duration. The AIP should not send a false signal during those cases. In order to avoid a fault triggering during those cases, a time delay TD with (10) and (11) is introduced. When the reactive power mismatch in (10) is satisfied for TD time, and (11) and/or (13) are satisfied, the proposed AIP scheme considers the inverter in an islanding condition.

D. IMPLEMENTATION SUMMARY

Based on the mathematical modeling in the previous subsections, the AIP scheme can be presented through a flowchart as shown in Fig. 2 and can be implemented in a digital controller as shown in Fig. 3. The reactive power mismatch exceeds the threshold limit QL for a delay time TD. The delay time should be set according to the standard grid code requirement. In addition, the active power and/or voltage magnitude mismatch exceed their threshold limits PL and VL, then

AIP scheme recognizes the situation as an islanding condition and the islanding detection signal (IDS) will be 1 (high) in in the logic circuit shown in Fig. 3.

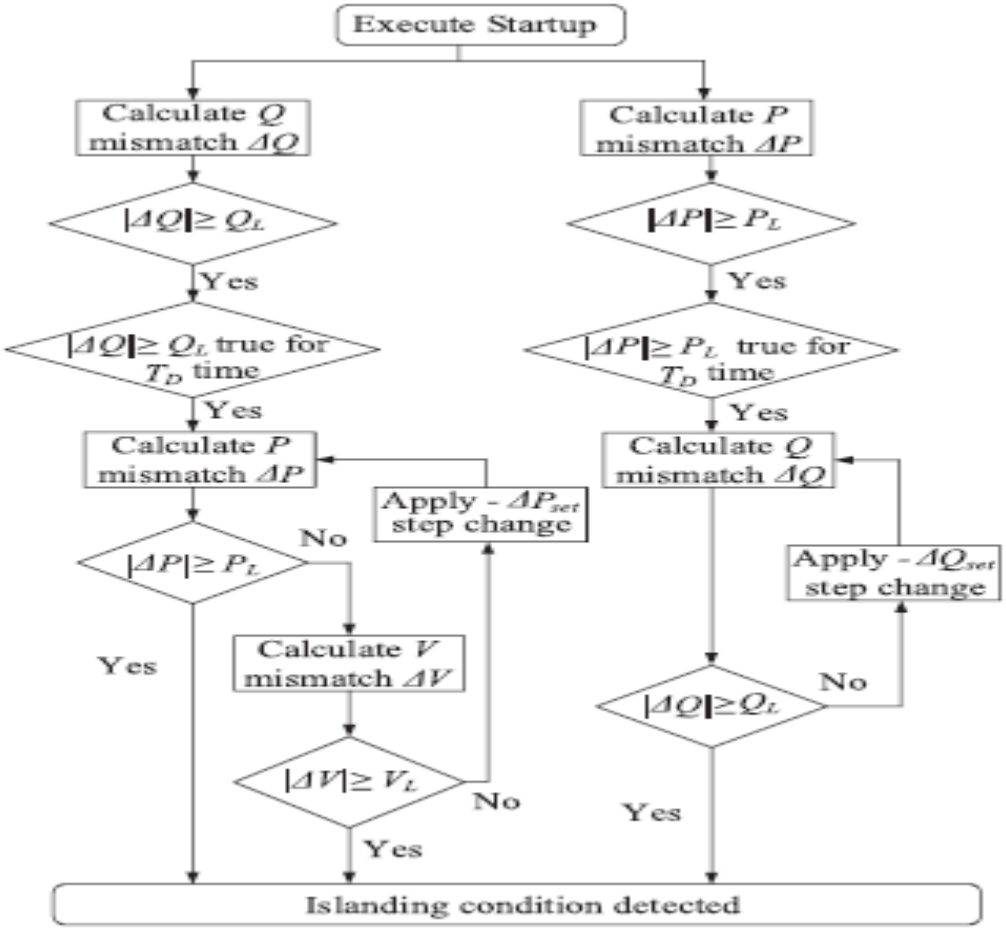

FIGURE 5. Flowchart of the proposed AIP scheme.

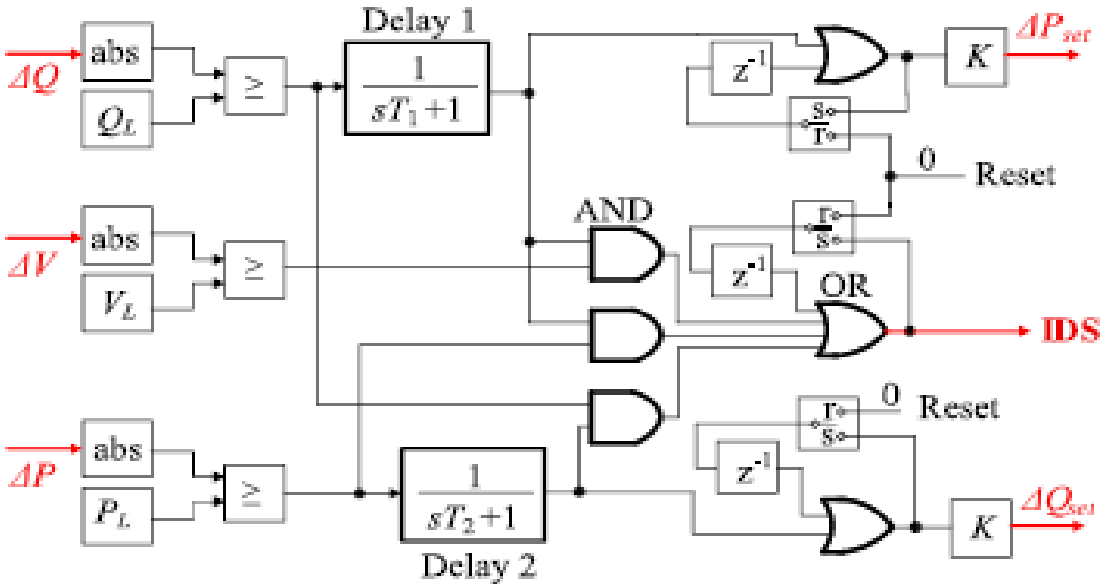

FIGURE 6. Control block diagram of the proposed AIP scheme.

The working procedure of the AIP scheme for the critical case scenarios is summarized in the following.

- If the reactive power mismatch exceeds the threshold limit QL for the duration of the delay time TD but the active power or the voltage magnitude mismatch does not exceed the threshold limits, PL and VL, the AIP will send a command signal to change Pset and then re-calculate the ΔP. If the new power mismatch exceeds limit PL, then AIP scheme recognizes the situation as an islanding condition.

TABLE 2. Parameters of the Investigated System

Parameters	Values
Rated apparent power, S_b	20 kVA
Rated grid voltage(L-L, RMS), V_o	208 V
Rated dc voltage,V_{dc}	500 V
Grid frequency, f	60 Hz
Inverter series inductance, L_c	1.4 mH
Inverter series resistance, R_c	0.1082 Ω
Filter capacitance, C_f	22 μF
Filter inductance, L_f	0.2295 mH
Filter parasitic resistance, R_f	0.1082 Ω
Virtual resistance, R_v	1 Ω
Constant, K_e	5

- If the reactive power mismatch does not exceed the threshold limit QL for the duration of the delay time TD but the active power mismatch exceeds the threshold limits, PL for the duration of the delay time TD, the AIP will send a command signal to change Qset and then re-calculate the ΔQ. If the new power mismatch exceeds limit QL, then AIP scheme recognizes the situation as an islanding condition. As can be seen in Fig. 3, it has three OR gates. Once the output of the OR gates becomes one (high), they hold it to high. When the inverters are reconnected to the grid after the grid is recovered, it is necessary to make the output low again. These reset blocks are used to make the output low again when the DG inverters are reconnected to the grid. When the proposed method is used, it needs to pay attention to selecting the current signal for calculating the inverter output power. As can be seen in fig. 1, it must be the inverter current, ic which we used for calculating the active and reactive power. If the current io is used for calculating power, the method may not detect all islanding conditions, especially it may fail the detecting critical case scenario.

CHAPTER 4

SIMULATION AND RESULTS

The AIP scheme has been implemented to a control of a DG inverter as shown in Fig. 4. The robust droop control (RDC) VSM proposed in [33] is used to control the DG inverter. Fig. 5 depicts the control stage of the RDC with embedded AIP scheme. As can be seen in Fig. 5, the required input signals ΔP, ΔQ, ΔV for implementing the AIP are readily available from the RDC controller. The RDC can be implemented in a single-phase as well as three-phase inverter without much modification in the control. Details about the mathematical modeling and operation of the RDC can be found in [33]. The control of the bidirectional dc-dc converter with the energy storage is used to regulate the dc-bus voltage. The system shown in Fig. 4 is implemented in MATLAB/ Simulink in association with Sim Power System block set. The parameters of the system are given in Table 1. The value of the threshold parameters QL, PL and VL has been decided how conservative the detection method should perform. Here, the threshold limits are set to QL = 0.1 pu, PL = 0.1 pu and VL = 0.1 pu. The time delay TD is set such that if the input to the transfer function is 1, the delay to reach the output 1 is 0.75 s. This means the AIP scheme detects an islanding condition in 0.75 s. Several simulations have been carried out for different scenarios to verify the effectiveness of the proposed AIP scheme. The simulation scenarios are divided into two categories, i) no false signal generated (subsection III-A and III-B) and ii) an IDS generated (subsection III-C) when an islanding occurs. The simulation scenarios are described in the following.

A. CHANGE OF THE POWER REFERENCE

The first simulation has been carried out for a normal operation with a command signal for changing Pset and Qset. No islanding condition is initiated. The time domain responses are shown in Figure 8. Initially, the inverter is operating in self-synchronization mode [33]. At 0.5 s, The grid connection circuit breaker (CB 1) has been closed and at the same time, the control mode of the VSM is changed from the selfsynchronization mode to the droop-mode with Pset = 0 and Qset = 0. The connection to the grid at 0.5 s is very smooth with a small transient. At 1 s, the real power and reactive power commands are set to Pset = 15 kW and Qset = 3 kVar and the inverter quickly responded to the commands accurately. Another command is given at 3 s to change Pset from 15 kW to 10 kW. The inverter follows the given command smoothly. The IDS is 0 during this

operation as shown in the bottom plot of Fig 8, meaning an islanding condition is not occurred/detected.

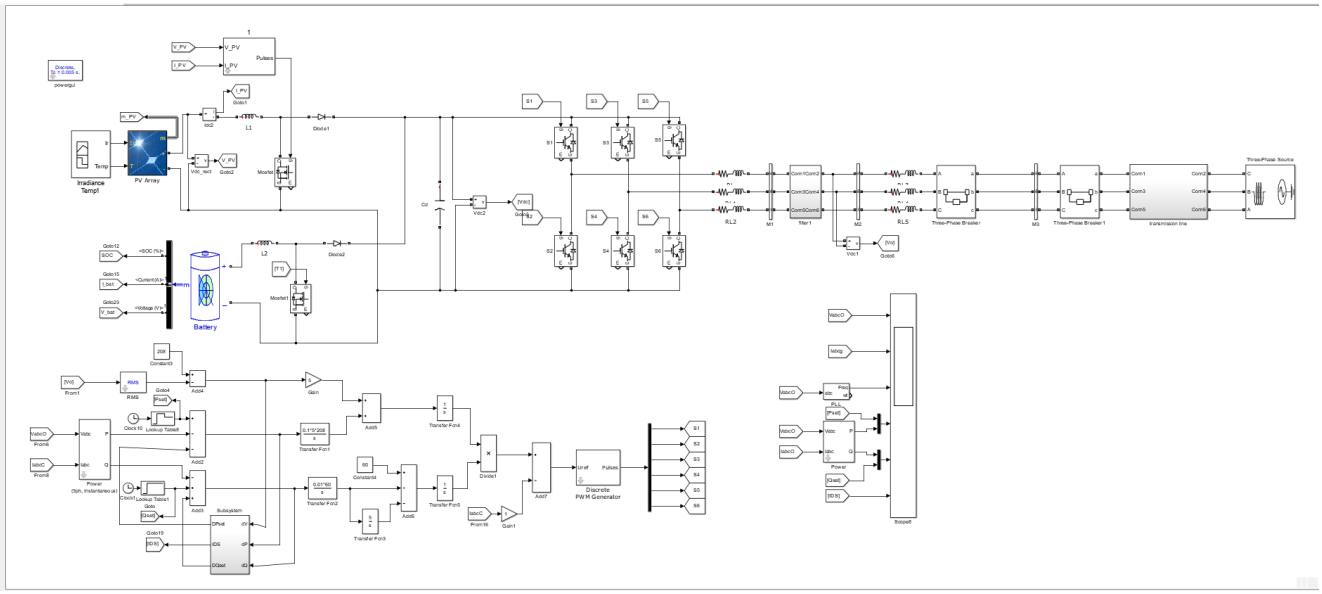

Figure 7.Simulation of the proposed model

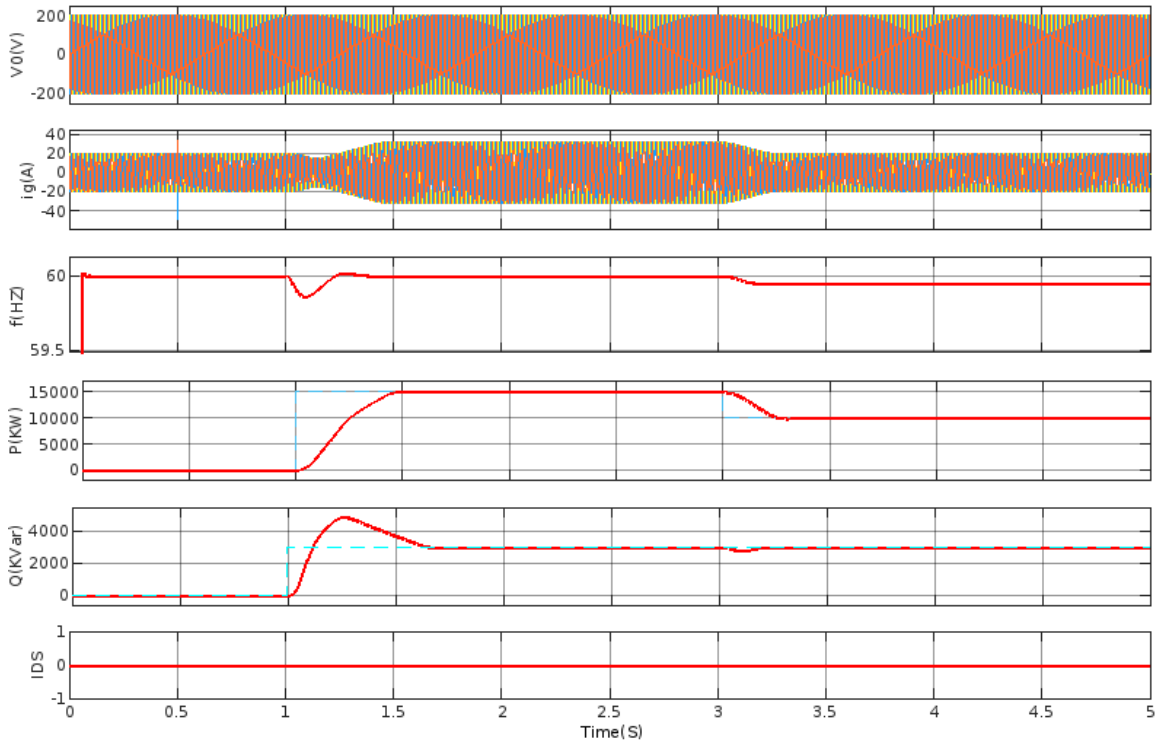

Figure 8.Simulation results of change of the power reference

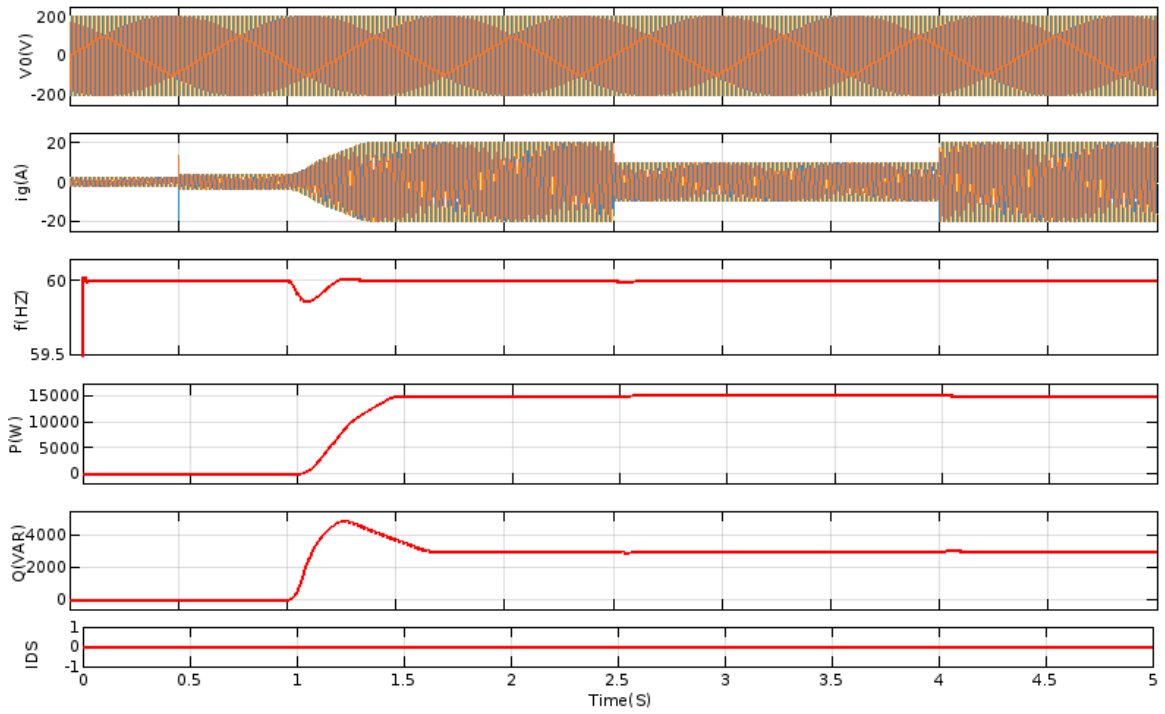

Figure 9.Simulation results of Islanding occuring when the load is connected and disconnected

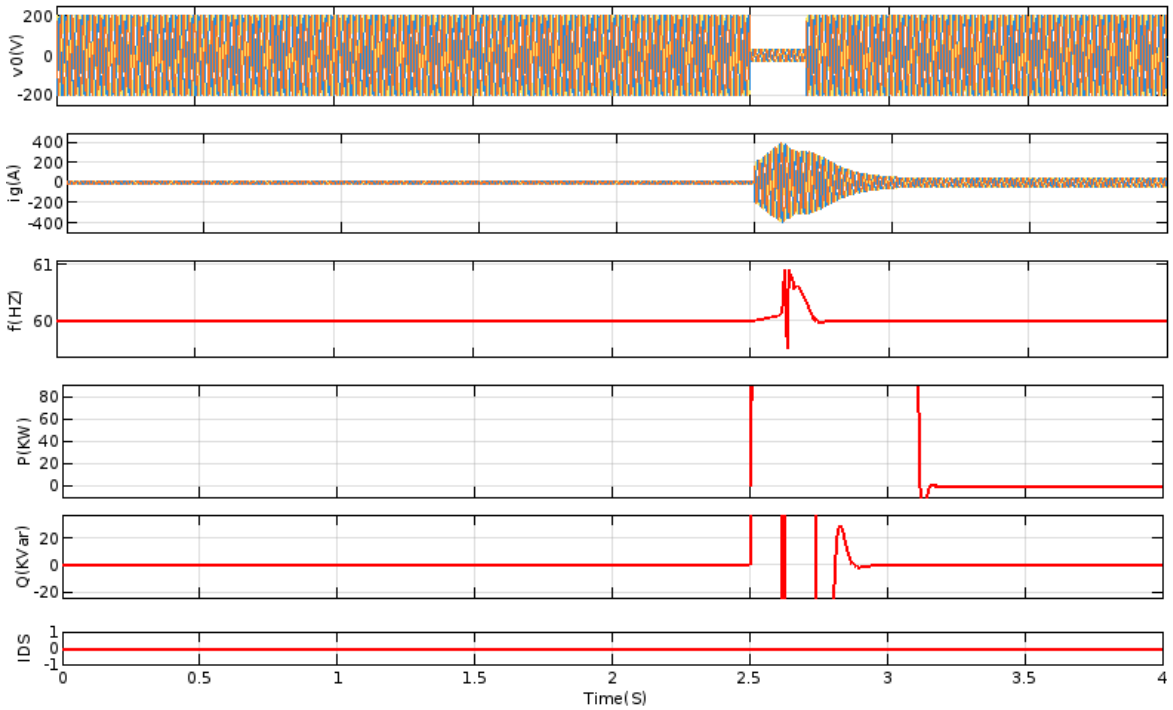

Figure 10.Simulation results of Islanding occuring when there is fault in the grid

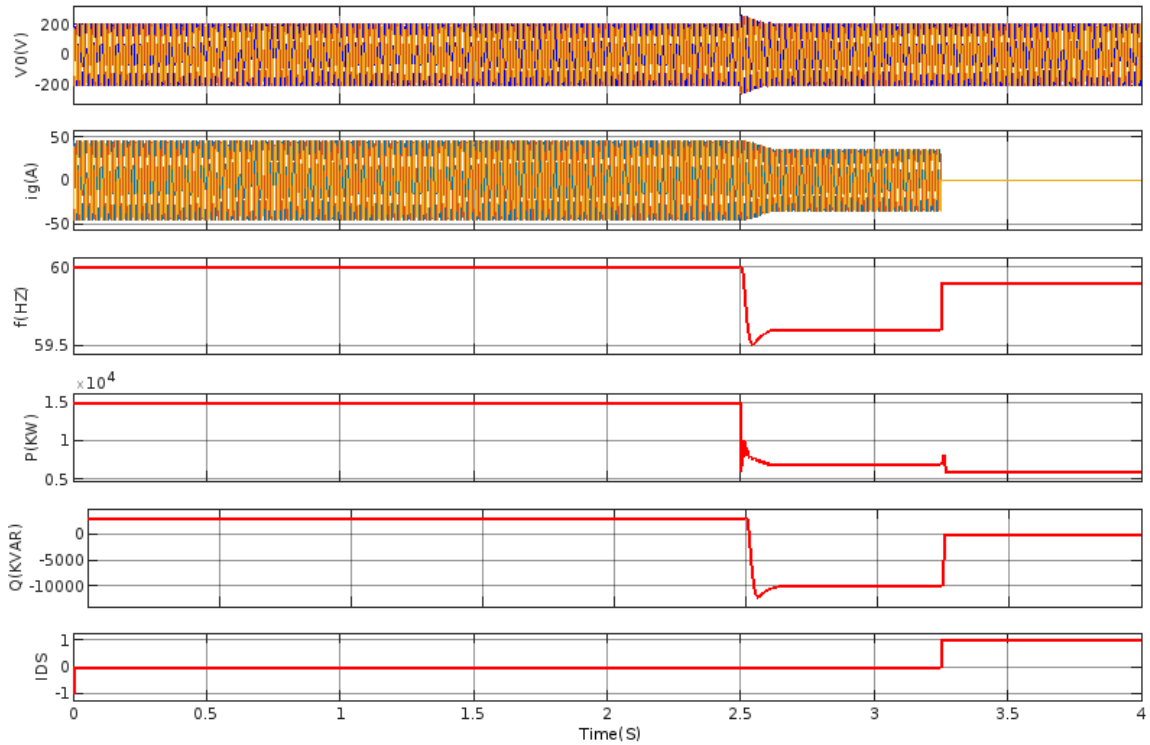

Figure 11.Simulation results of Islanding occuring when the local load is smaller that Pset. Pset=15KW and Pload=5KW.

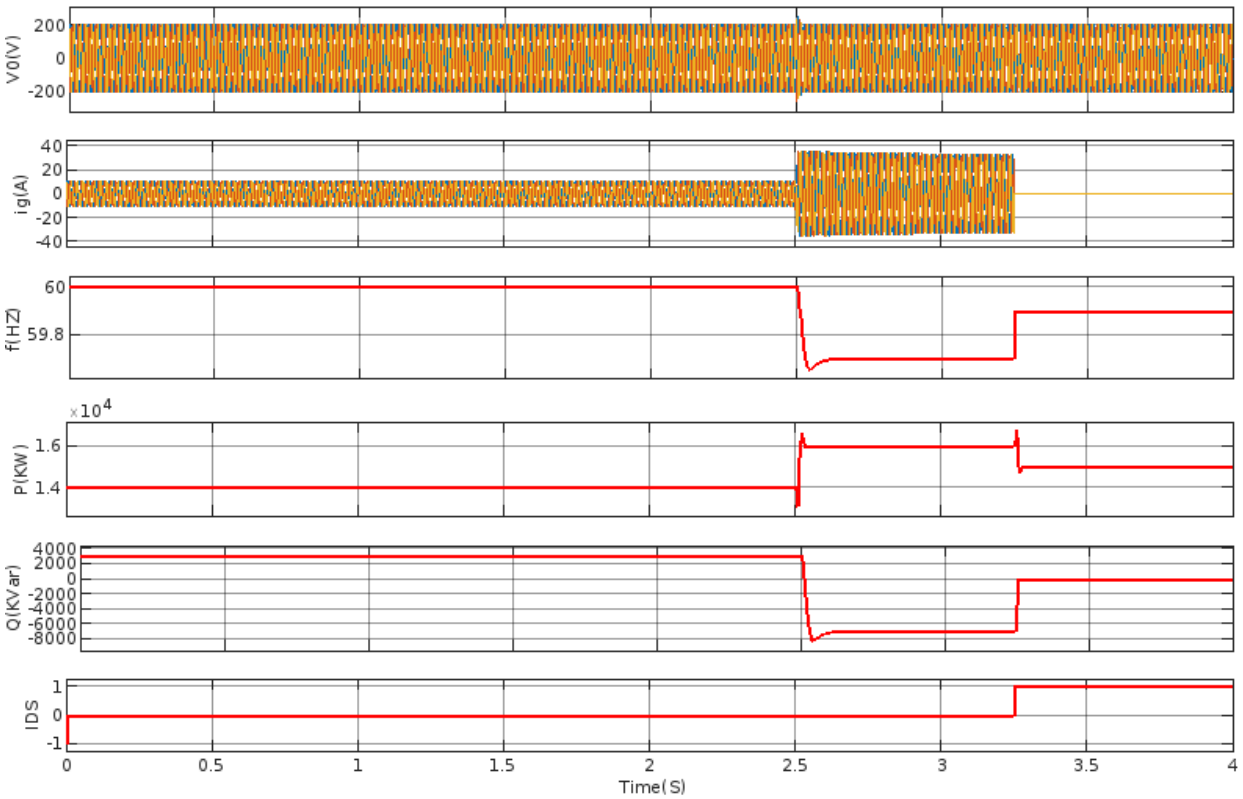

Figure 12.Simulation results of Islanding occuring when the local load is equal to Pset. Pset=Pload=15KW.

B.A HIGH LOAD CONNECTION/DISCONNECTION AND A GRID FAULT

A load connection/disconnection and a fault have been simulated to investigate the performance of the AIP scheme. A load change has been tested by connecting and disconnecting a 20-kW of a local load. Fig. 9 shows the simulation results for the case when the 20-kW load is connected to the grid at 2.5 s and disconnected at 4.0 s. During this load connection and disconnection, the inverter is acting according to its dynamic droop setting to support the grid. The IDS remains 0 and no islanding condition is detected. Fig. 10 shows the simulation results for a three-phase to ground fault. The fault has been initiated at 2.5 s and cleared after 5 cycles. The power and voltage mismatch exceed the threshold limits during the fault, however, they are recovered when the fault is cleared. The IDS remains 0 and no islanding condition is detected. Hence, the AIP scheme does not generate a false signal during a grid fault.

C.ISLANDING OCCURRED AT DIFFERENT LOADING CONDITION OF THE LOCAL LOAD

These simulations have been carried out for different local load power while an islanding condition occurs. The first scenario is when the local load is less than the power send by the inverter. Pset and Qset are 15 kW and 3 kVar, respectively. The local load is 5 kW. The simulation results are shown in Fig. 11. Initially, the system operates in the grid-connected mode and the IDS is zero. At 2.5 s, an islanding condition occurs. As can be seen in the bottom plot of Fig. 11, the IDS becomes 1 at 3.25 s. The islanding condition is detected after 0.75 s of actual islanding occurred which is the specified time, 0.75 s set by the AIP designer. The system is designed such a way that when the IDS becomes 1, then CB 2 is opened to isolate the inverter from the rest of the grid. As can be seen, the current to the grid ig becomes zero at 3.25 s since CB 2 is opened. After isolation at 3.25 s, the inverter operates in the stand-alone mode and supplies power to the local load. Another simulation has been carried out for the case when the local load is equal to the power supplied by the inverter. The time domain responses are shown in Fig. 12. Pset and Qset are 15 kW and 3 kVar. The local load is equal to Pset. In order to comply with IEEE 1547 Standard [7], in addition to a resistive load, the load network contains a 15-kVar capacitive and a 15-kVar inductive elements that cancel each other out. This creates a self-resonating island. Initially, the system is operating in the grid-connected mode, there is no violation of the threshold limit until 2.5 s. At 2.5 s, an islanding condition occurs. The reactive power mismatch $|\Delta Q|$ has exceeded the threshold limit QL when the active power mismatch $|\Delta P|$ and the voltage mismatch $|\Delta V|$ do not exceed the threshold limits PL and VL since Pset = Pload and the inverter regulates the voltage. During the time from 2.5 s to 3.25 s, only the reactive power mismatch exceeds the limit QL. Since no violation occurs except the reactive power mismatch for 0.75 s duration, the AIP generates a command signal to change Pset for a step of $\Delta P_{set} = 0.125$ pu at 3.25 s. For this change of Pset , the active power mismatch $|\Delta P|$ exceeds the threshold limit PL. Thus, (10), and (11) are satisfied. The IDS becomes 1 as shown in the bottom plot of Fig. 12. The islanding condition is detected. Hence, CB 2 operates to isolate the inverter from the rest of the grid. After isolation, the inverter operates in the islanding-mode and supplies stable power to the local load. The proposed AIP scheme works properly and can successfully detect the islanding condition.

CHAPTER 5

CONCLUSION

This paper presents a novel hybrid AIP scheme for DG inverters. The implementation of the AIP scheme is based on the signal obtained from the DG inverter controller. The main advantage of this proposed AIP scheme is that it can be embedded into the control of inverters without a need of additional part in the hardware of the inverter and any change in the controller. The proposed AIP scheme does not rely on the communication network and is based on the local measurements. It detects the islanding condition based on continuous monitoring of the active power, the reactive power, and the voltage magnitude mismatch, which is shown to be an alternative to the impedance variation measurement technique. The complicated disturbance injection method in active method has been avoided, consequently, the risk of triggering instability and power quality issues has been eliminated as well as, it overcomes the malfunctioning of passive methods when the local load is equal to the power supplied by the inverter. The AIP scheme is tested under all possible islanding cases. Simulation and experimental results have verified the islanding detection function of the proposed AIP scheme.

CHAPTER 6

REFERENCES:

[1] S. D'Arco and J. A. Suul, "Equivalence of virtual synchronous machines and frequency-droops for converter-based microgrids," IEEE Trans. Smart Grid, vol. 5, no. 1, pp. 394–395, Jan. 2014.

[2] J. Zhu, C. D. Booth, G. P. Adam, A. J. Roscoe, and C. G. Bright, "Inertia emulation control strategy for VSC-HVDC transmission systems," IEEE Trans. Power Syst., vol. 28, no. 2, pp. 1277–1287, May 2013.

[3] D. Duckwitz and B. Fischer, "Modeling and design of df /dt -based inertia control for power converters," IEEE J. Emerg. Sel. Topics Power Electron., vol. 5, no. 4, pp. 1553–1564, Dec. 2017.

[4] S. D'arco, J. A. Suul, and O. B. Fosso, "A virtual synchronous machine implementation for distributed control of power converters in smartgrids," Electric Power Syst. Res., vol. 122, pp. 180–197, May 2015.

[5] Q.-C. Zhong, "Robust droop controller for accurate proportional load sharing among inverters operated in parallel," IEEE Trans. Ind. Electron., vol. 60, no. 4, pp. 1281–1290, Apr. 2013.

[6] M. Amin and Q.-C. Zhong, "Resynchronization of distributed generation based on the universal droop controller for seamless transfer between operation modes," IEEE Trans. Ind. Electron., vol. 67, no. 9, pp. 7574–7582, Sep. 2020.

[7] Interconnecting Distribution Resources Electric Power System, IEEE Standard 1547, 2003.

[8] H. Laaksonen, "Advanced islanding detection functionality for future electricity distribution networks," IEEE Trans. Power Del., vol. 28, no. 4, pp. 2056–2064, Oct. 2013.

[9] J. C. M. Vieira, W. Freitas, W. Xu, and A. Morelato, "An investigation on the nondetection zones of synchronous distributed generation antiislanding protection," IEEE Trans. Power Del., vol. 23, no. 2, pp. 593– 600, Apr. 2008.

[10] F. D. Mango, M. Liserre, A. Dell'aquila, and A. Pigazo, "Overview of anti-islanding algorithms for PV systems. Part I: Passive methods," in Proc. 12th Int. Power Electron. Motion Control Conf., Aug. 2006, pp. 1878–1883.

[11] F. D. Mango, M. Liserre, and A. Dellaquila, “Overview of anti-islanding algorithms for PV systems,” in Proc. 12th Int. Power Electron. Motion Control Conf., Aug. 2006, pp. 1884–1889.

[12] X. Wang and W. Freitas, “Impact of positive-feedback anti-islanding methods on small-signal stability of inverter-based distributed generation,” IEEE Trans. Energy Convers, vol. 23, no. 3, p. 923931, Sep. 2008.

[13] Y. Zhou, H. Li, and L. Liu, “Integrated autonomous voltage regulation and islanding detection for high penetration PV applications,” IEEE Trans. Power Electron., vol. 28, no. 6, pp. 2826–2841, Jun. 2013.

[14] M. Bayrak, “Recurrent artificial neural network based islanding protection by using generator speed deviation,” Scientific Res. Essay, vol. 4, no. 4, pp. 212–216, Apr. 2009.

[15] M. S. Elnozahy, E. F. El-Saadany, and M. M. A. Salama, “A robust wavelet-ANN based technique for islanding detection,” in Proc. IEEE Power Energy Soc. General Meeting, Jul. 2011, p. 18.

[16] A. Pouryekta, V. K. Ramachandaramurthy, N. Mithulananthan, and A. Arulampalam, “Islanding detection and enhancement of microgrid performance,” IEEE Syst. J., vol. 12, no. 4, pp. 3131–3141, Dec. 2018.

[17] X. Chen, Y. Li, and P. Crossley, “A novel hybrid islanding detection method for grid-connected microgrids with multiple inverter-based distributed generators based on adaptive reactive power disturbance and passive criteria,” IEEE Trans. Power Electron., vol. 34, no. 9, pp. 9342– 9356, Sep. 2019.

[18] M. R. Alam,M. T. A. Begum, and K. M. Muttaqi, “Assessing the performance of ROCOF relay for anti-islanding protection of distributed generation under subcritical region of power imbalance,” vol. 55, p. 5395– 5405, Sep. 2018.

[19] J. Ke, Z. Zhengxuan, Z. Qijuan, Y. Zhe, and B. Tianshu, “Islanding detection method of multi-port photovoltaic DC micro grid based on harmonic impedance measurement,” IET Renewable Power Generation, vol. 13, no. 14, pp. 2604–2611, Oct. 2019.

[20] M. Amin, Q.-C. Zhong, Z. Lyu, L. Zhang, Z. Li, and M. Shahidehpour, “An anti-islanding protection for inverters in distributed generation,” in Proc. IECON - 44th Annu. Conf. IEEE Ind. Electron. Soc., Oct. 2018, pp. 1669–1674.

[21] N. B. Hartmann, R. C. D. Santos, A. P. Grilo, and J. C. M. Vieira, “Hardware implementation and real-time evaluation of an ANN-based algorithm for anti-islanding

protection of distributed generators," IEEE Trans. Ind. Electron., vol. 65, no. 6, pp. 5051–5059, Jun. 2018.

[22] B.-G. G. Yu, M. Matsui, and G.-J. G. Yu, "A correlation-based islanding-detection method using current-magnitude disturbance for PV system," IEEE Trans. Ind. Electron., vol. 58, no. 7, pp. 2935–2943, Jul. 2011.

[23] J.-H. H. Kim, J.-G. H. Kim, Y.-H. H. Ji, Y.-C. C. Jung, and C.-Y. Y.Won, "An islanding detection method for a grid-connected system based on the Goertzel algorithm," IEEE Trans. Power Electron., vol. 26, no. 4, pp. 1049–1055, Apr. 2011.

[24] L. Asiminoaei, R. Teodorescu, F. Blaabjerg, and U. Borup, "A digital controlled PV-inverter with grid impedance estimation for ENS detection," IEEE Trans. Power Electron., vol. 20, no. 6, pp. 1480–1490, Nov. 2005.

[25] P. Gupta, R. S. Bhatia, and D. K. Jain, "Active ROCOF relay for islanding detection," IEEE Trans. Power Del., vol. 32, no. 1, pp. 420–429, Feb. 2017.

[26] O. Raipala, A. S. Makinen, S. Repo, and P. Jarventausta, "An antiislanding protection method based on reactive power injection and ROCOF," IEEE Trans. Power Del., vol. 32, no. 1, pp. 401–410, Feb. 2017.

[27] S. A. Saleh, A. S. Aljankawey, R. Meng, J. Meng, L. Chang, and C. P. Diduch, "Apparent power-based anti-islanding protection for distributed cogeneration systems," IEEE Trans. Industry Appl., vol. 52, no. 1, pp. 83–98, Jan. 2016.

[28] Y. Si, Y. Liu, C. Liu, Z. Zhang, and Q. Lei, "Reactive power injection and SOGI based active anti-islanding protection method," in Proc. IEEE Energy Convers. Congr. Expo. (ECCE), Sep. 2019, pp. 2637–2642.

[29] A. G. Abokhalil, A. B. Awan, and A.-R. Al-Qawasmi, "Comparative study of passive and active islanding detection methods for PV gridconnected systems," Sustainability, vol. 10, no. 6, p. 1798, May 2018.

[30] M.-S. Kim, R. Haider, G.-J. Cho, C.-H. Kim, C.-Y.Won, and J.-S. Chai, "Comprehensive review of islanding detection methods for distributed generation systems," Energies, vol. 12, no. 5, p. 837, Mar. 2019.